Mammalian Gene Circuits

Introduction

Synthetic biology, a relatively new field founded in the early 2000s, implements molecular biology tools to forward-engineer cellular behaviour, allowing researchers to modify organisms to work for their benefits. A very promising example of this is creating logical gates using genetic circuits [1]. An essential step in implementing these circuits is however encoding a biological process to be able to perform further downstream computations. An example of this can be found in a 2016 paper by Angelici et al. [2], designing a sensor module as seen in figure 1.

In this practical course, we attempted to reproduce these results. This included transfecting Hek293 TetON cells with i) a transcription factor (in our case SOX10) under the control of a Tet-responsive element (TRE) as an input with mCherry as a proxy and ii) either an open-loop amCyan output under a SOX10 response element, or a feedback-loop amCyan output also induced by SOX10, but also containing positive feedback due to the additional PIR element and the expression of PIT2 when activated. The resulting cell populations were characterized using microscopy and flow cytometry.

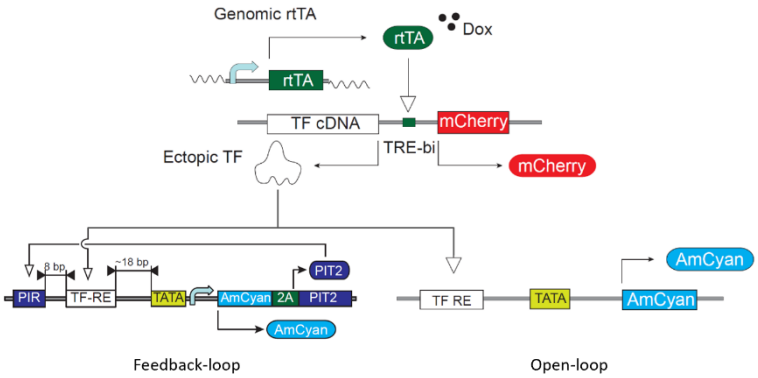

Figure 1: Cartoon presentation of the sensor circuit in the Hek293 TetON cell line. The ectopic transcription factor expressed under the TRE is SOX10 in this case. In each cell there is only either the feedback- (left) or open-loop (right) plasmid, both expressing AmCyan as the output. *Adapted from* [2]

Materials & Methods

Plasmids

Table 1: Plasmids used for circuit (pBA477, pBA480 & pBA417), controls (pKH025, pKH026, pBA008), as well as filler DNA (pBH265), including a short description of the plasmids construct.

Plasmid	Construct	Description
pBA477	PIR-3xC-C SOX10 RE-amCyan_intron-2A-PIT2 feedback loop	SOX9/10 feedback loop sensor: amCyan & PIR under minimal TATA promoter regulated by SOX9/10 & PIT2 responsive element; PIR binds to PIT2, inducing transcription and leading to positive feedback
pBA480	PIR-3xC-C SOX10 RE-amCyan_intron-2A-mutated_PIT2 open loop	SOX9/10 open loop sensor: amCyan & PIR under minimal TATA promoter regulated by SOX9/10 responsive element; PIT2 is mutated to prevent PIR induction
pBA417	SOX10-bi_TRE-mCherry	SOX10 & mCherry under Bidirectional Tet-Responsive Element (TRE) promoter
pKH025	prEF1α-Citrine	Citrine under constitutive prEF1α promoter; transfection control
pKH026	prEF1α-mCherry	mCherry under constitutive prEF1α promoter; transfection control
pBA008	prEF1α-amCyan	amCyan under constitutive prEF1α promoter; transfection control
pBH265	prUbi; NOS terminator	'Junk' DNA; used as filler plasmid in transfection controls

Plasmid Purification

For each plasmid (except for pBA008), 50 ml of the E.coli TOP10 overexpression cultures were lysed and the plasmids purified with the Pureyield Plasmid Midiprep System according to the protocol:
The cells were spun down and the supernatant discarded before resuspension in lysis buffer and incubated. Lysis was stopped by adding neutralization buffer and spun down after another incubation step. The supernatant was transferred onto the Midiprep column and washed with endotoxin removal and standard column wash buffer. The plasmids were then eluted with nuclease-free water.
To further reduce the lipopolysaccharide (LPS) endotoxin concentration, the resulting plasmid solutions were treated with the Norgen Endotoxin Removal Kit, again following the protocol:
Buffer SK and endotoxin removal buffer were added to the plasmid solution and incubated before adding isopropanol and transferred to the column. Flow through was discarded and the column washed before eluting the plasmids with 600 µl elution buffer.

Plasmid restriction digest

400 ng of each plasmid was (from the endotoxin free solution) was added to 2.5 µl 10x fast digest buffer. For the quantification digest, 1 µl of the respective restriction enzyme was added, while 0.75 µl of each enzyme was added to the solution. The resulting solution was filled up to 25 µl with dH_2O. The restriction digest was incubated for over 60 min at 37˚C, before deactivating the restriction enzymes by incubating at 80˚C for 15 min.

Agarose gel electrophoresis

The 1% w/v agarose gel was made by adding 1 g of agarose to 100 ml of 1x TAE buffer. The solution was heated in the microwave and let to cool before adding 10 µl SYBR Safe. The solution was added into a tray and a comb was added for the wells. The gel was run at 120V for ~1h.

Gel quantification

Gels were photographed using an exposure time of 2 s, and lane intensities were quantified and plotted using ImageJ. The bands were then quantified by selecting peaks and measuring the area under curve.
To determine the DNA amounts in plasmid samples, different volumes of 1kb DNA ladder with 0.1 µg/µl were added and a standard curve calculated by adding a linear fit to the 1kb band of the ladder (see figure 4). The plasmid values were then determined by multiplying band intensities with the slope.

Cell Seeding

HEK293 TetON cells were used for transfection of circuit and control plasmids. Pre-cultured cells in T-75 cell culture flasks were extracted by first removing medium, washing with 10 ml 1x phosphate buffered saline (PBS), and then detaching them from the surface by adding 5 ml of 0.25% Trypsin-EDTA. 20 µl of the resulting cell solution was stained with Trypan blue and cells were counted using a TC-10 cell counter. The cells were then diluted in medium to achieve a final solution of $2*10^5$ cells/ml (Table 2). From this solution, 0.5 ml was added into each well of the 24-well plate (Figure 2). The process was repeated for a second plate, one for the feedback and one for the open loop transfection.

Table 2: Values resulting from TC-10 cell counter and following calculations to achieve the desired solution.

Loop	Cell count/ml	Desired dilution (cells/ml)	Volume cell suspension dilution (ml)	Volume medium dilution (ml)	Volume per well (ml)
Open	$1.88*10^6$	$2*10^5$	2.128	17.872	0.5
Feedback	$2.495*10^6$	$2*10^5$	1.603	18.397	0.5

Cell Transfection

The cells were transfected 17 h after seeding, incubated at 37˚C and 0.5% CO_2. 100 µl of medium was removed from each well and 100 µl of doxycycline solution with the right concentration was added to achieve the correct final concentration in each well. Finally, 100 µl of the corresponding plasmid-lipofectamine solutions were added into each well. Further calculations and a thorough transfection plan can be found in supplementary figures S1/2.

Table 3: DNA amounts for each well, always summing up to 440 ng. Lipofectamine was added to every sample at a 1:2 ratio, i.e. 880 nl for each well. The solution was filled to 100 µl with OptiMEM.

	pBA480/477 [ng]	pBA417 [ng]	pKH025 [ng]	pKH026 [ng]	pBA008 [ng]	pBH265 [ng]
Circuit	120	120	200	-	-	-
AmCyan Ctrl.	-	-	-	-	120	320
mCherry Ctrl.	-	-	-	120	-	320
Citrine Ctrl.	-	-	120	-	-	320
OptiMEM Ctrl.	-	-	-	-	-	-

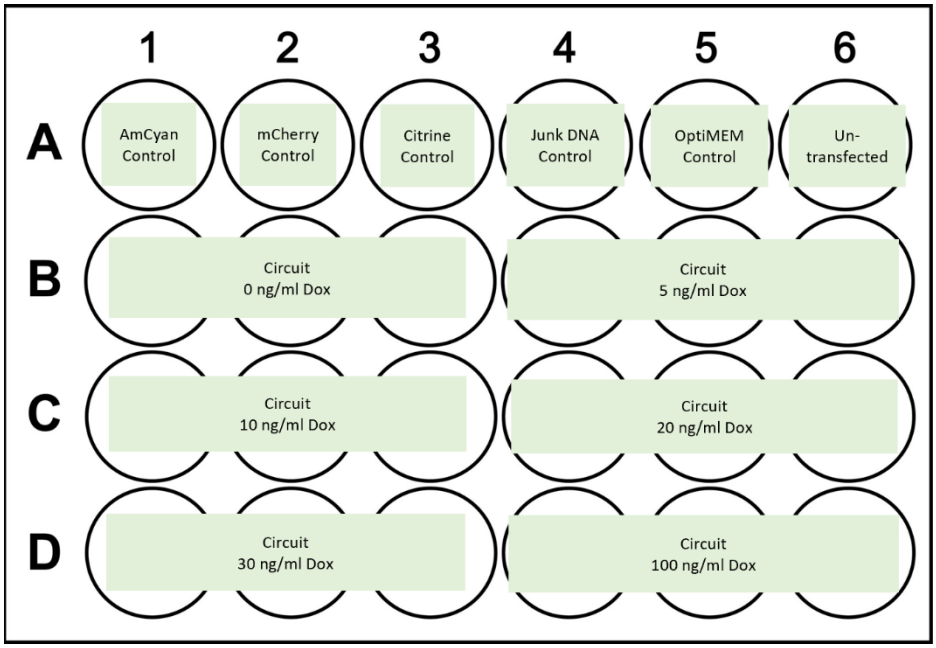

Figure 2: Transfection plan of 24 well plate. All single-colour and negative controls were seeded in row A, and circuit DNA (feedback and open loop respectively) with varying concentrations of doxycycline. Three replicates were seeded for each doxycycline concentration.

Fluorescence Microscopy

Images were taken for every well at 10x magnification in bright-field and all three fluorescent channels. For the bright-field, 10 s exposure time and standard 10x phase settings were used. For the fluorescent channels, the respective filter sets were used (amCyan: CFP setting; mCherry: Cy3 settings; Citrine: YFP settings), and images were taken for three different exposure times (100 s, 300 s, 500 s). The images were evaluated and edited using NIS viewer and ImageJ FIJI.

Flow Cytometry

For flow cytometry, the medium was removed from the wells before resuspending the cells in accutase to detach the cells. Cells were then measured on a BD Fortress flow cytometer with settings as seen in table 4 and recorded until 150’000 cells were reached or the medium was depleted. Area, height, and width of measurement peaks were exported and analysed using FlowJo.

For the analysis, the cells were gated for single live cells using forward (FSC) and side (SSC) scattering. Spill over of fluorescent signal was compensated from amCyan to Citrine (Feedback: 0.078, Open: 0.017) and Citrine to mCherry (Feedback: 0.003, Open: 0.003).
The fluorescence intensities of the resulting populations were then documented (see figure 6) and gated for positive hits. The frequency of parent and mean of this final population was exported and the integrated fluorescence intensities calculated (freq. of par. multiplied with mean) (see figure 7).

Table 4: Settings used for different acquisition methods, including photomultiplier values for all channels and excitation and filter set for fluorescent channels.

Acquisition	PMTs (mV)	Excitation Laser	Filter set
FSC	367	-	-
SSC	210	-	-
AmCyan	255	Bv 445 nm	E 473/10
mCherry	210	Blue 488 nm	C 542/27 & LP 505
Citrine	210	Yellow/Green 561 nm	D 610/20 LP 600

Matlab analysis

Similar to analysis with FlowJo, cells were gated for single live cells & compensated for signal spill over. Five cut-offs were then drawn based off of Citrine intensity frequencies to define four bins of different general plasmid copy numbers, of which bin number 3 was chosen. The intensities of the peaks of histograms for amCyan and mCherry were determined using a bimodal fit, and these values plotted.
The experimental data was also compared to the simulated data, using a provided SimBiology model as seen in figure Sx. The simulation was tested for different plasmid copy numbers and transcription rates, of which the most similarnto the experimental data was chosen. To simulate single cells, the simulation was repeated several times with a certain level of noise. Scatter plots were also generated using this simulated data.

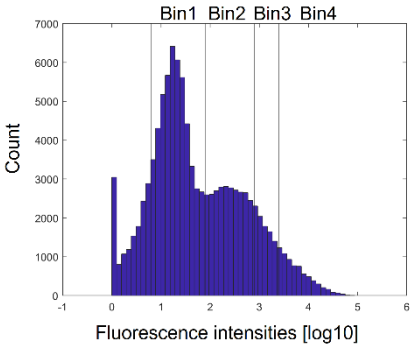

Figure 2: Representative histogram plot of citrine fluorescence values used for determining cut offs for bins. Cut off values (in log scale): [0.8, 1.9, 2.9, 3.4, 6].

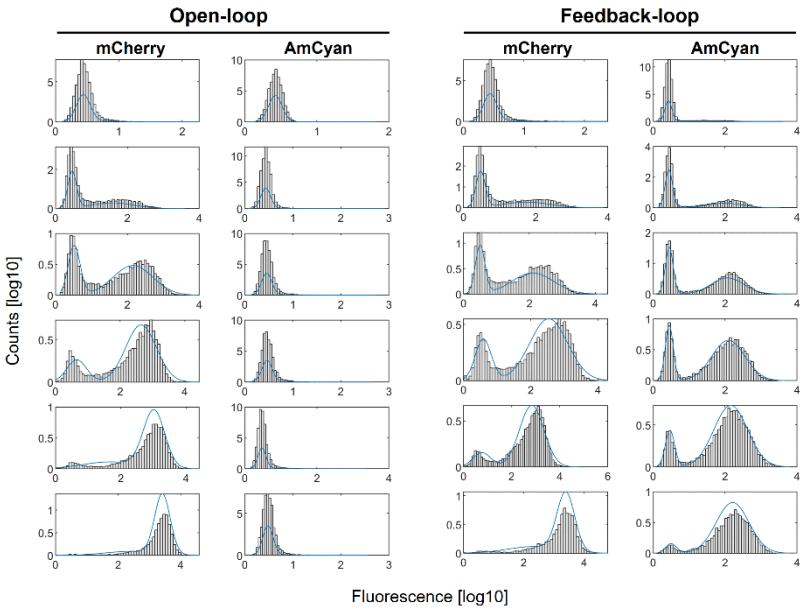

Figure 3: Demonstration of bimodal fitting to bin3 histograms. Peak values are tabulated in table S2.

Results

Plasmid Purification

Plasmid concentrations were measured on nanodrop before (in 500 µl) and after (in 600 µl) endotoxin removal, also measuring A260/280 & A260/230 ratios to confirm purity. Concentrations after endotoxin removal were also measured using gel quantification (Table 5).

We can see a larger amount of plasmid was lost in the endotoxin removal, reducing the yield from an average of 3.8 µg per ml of culture to 0.6 µg/ml. Also, while the A260/280 ratio stays similar, the A260/230 after endotoxin removal is notably lower than before. This is most likely due to some contaminants from the endotoxin removal buffer (such as guanidinium hydrochloride), which should however not be harmful towards the cells.

Additionally, we can see the gel quantification deviates slightly from the nanodrop, giving mostly lower concentrations. This can be explained by the fact that nanodrop measures the absorption of the solution with the plasmid, which can be influenced by contaminants or other DNA fragments, while the gel only considers the plasmid of interest. Gel quantification values were thus also used for calculations in the transfection plan.

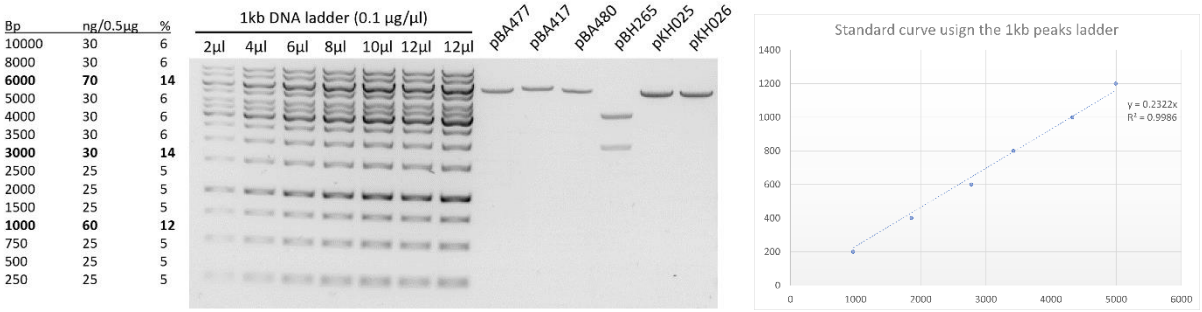

Figure 4: Agarose gel used for gel quantification. The standard curve was calculated using the 1000 bp band of the DNA ladder at the given plasmid amounts. Only the second 12 ul ladder value was used for standard curve calculation due to pipetting mistakes made on the first 12 ul ladder lane.
For pBH265 the wrong restriction enzyme was used which cut at two sites, leading to two different fragments. To correct for this, the sum of the integrals was used to determine the total concentration.

Table 5: Concentration values and absorption ratios of plasmids measured with Nanodrop after Midiprep & endotoxin removal, as well as gel quantification concentration values for the samples after endotoxin removal. pBA008 concentration values were provided by the supervisors.

	Nanodrop after Midiprep			Nanodrop after endotoxin removal			Final Gel Quantification
Plasmid	**Conc. [ng/µl]**	**Ratio A260/280**	**Ratio A260/230**	**Conc. [ng/µl]**	**Ratio A260/280**	**Ratio A260/230**	**Conc. [ng/µl]**
pBA477	204.2	1.91	1.98	32.7	1.85	0.24	22.6
pBA480	206.2	1.90	1.91	31.1	1.85	0.33	17.2
pBA417	169.9	1.92	1.85	26.5	1.83	0.28	16.4
pKH025	581.3	1.87	2.10	86.8	1.86	0.60	104.1
pKH026	489.8	1.90	2.14	50.5	1.85	0.24	56.6
pBA008	-	-	-	80.2	-	-	40
pBH265	609.4	1.88	2.14	73.7	1.85	0.64	67.2

Plasmid Verification

Plasmids were verified by i) sequencing the areas of interest on each primer and ii) comparing the expected and actual restriction digest for each plasmid.

Primers were chosen according to areas of interest on each plasmid, and then sequenced by Microsynth using automated Sanger sequencing. The sequencing data confirmed correct sequences for all essential components of the circuit and control plasmids. Primers used for sequencing can be found in table S2.

Restriction enzymes for plasmid verification were chosen as to produce three fragments of characteristic lengths, as written in table 6. The expected fragment lengths were then compared to the observed fragment lengths determined through agarose gel electrophoresis (Figure 5). These observed fragments corresponded to the expected lengths of their respective plasmids, with exception of pBA417, where an additional band can be seen at ~4000 bp, and pBH265, which show several bands above the largest expected fragment. These additional bands for both of the plasmids can however be explained by incomplete digestion, since their sizes correlate to combinations of the expected fragment lengths.

Table 6: list of restriction enzymes used for plasmid digestion and the expected fragment sizes. First listed restriction enzyme was also used in single digest for gel quantification.

Plasmid	Restriction enzymes	Expected fragments
pBA477	HindIII, PvuI	2859, 1553, 1045
pBA417	HindIII, PvuI, XbaI	3346, 1596, 744
pBA480	HindIII, XhoI	3165, 1253, 1039
pBH265	XbaI, XhoI	3209, 1304, 663
pKH025	HindIII, XhoI, XbaI	3519, 950, 553
pKH026	NotI, PvuI, XhoI	2514, 1552, 938

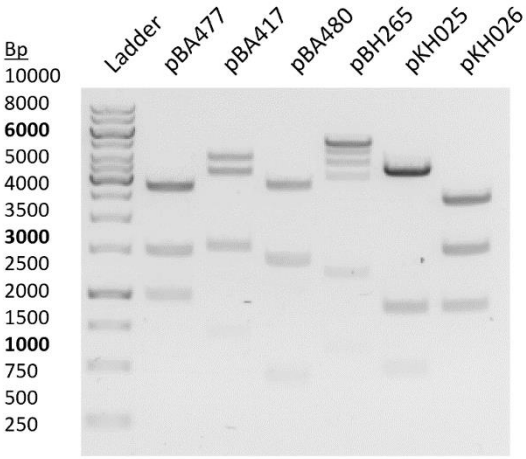

Figure 5: Plasmid verification gel. The same ladder was used as for the quantification. Bold bp numbers correspond to the darker ladder bands.

Transfection results

The integrity of the cells was checked under the microscope in the brightfield channel, showing densely packed and whole cells across all wells with exception of the amCyan colour control, where the cells had failed to adhere and formed a floating island. AmCyan signal was however still present, and the cells could thus be used (see Figure S9).

The wells were then photographed in all fluorescent channels as well, the results of which are seen in figure 6. As expected, Citrine levels stay mostly constant over all images, while mCherry increases with higher doxycycline concentrations. In the feedback-loop we can also see the amCyan increasing with higher doxycycline concentrations, the signal in the open loop is however not strong enough to be visible when comparing to the feedback-loop. There is also no obvious increase in amCyan in the open-loop even at maximum exposure time and high brightness.

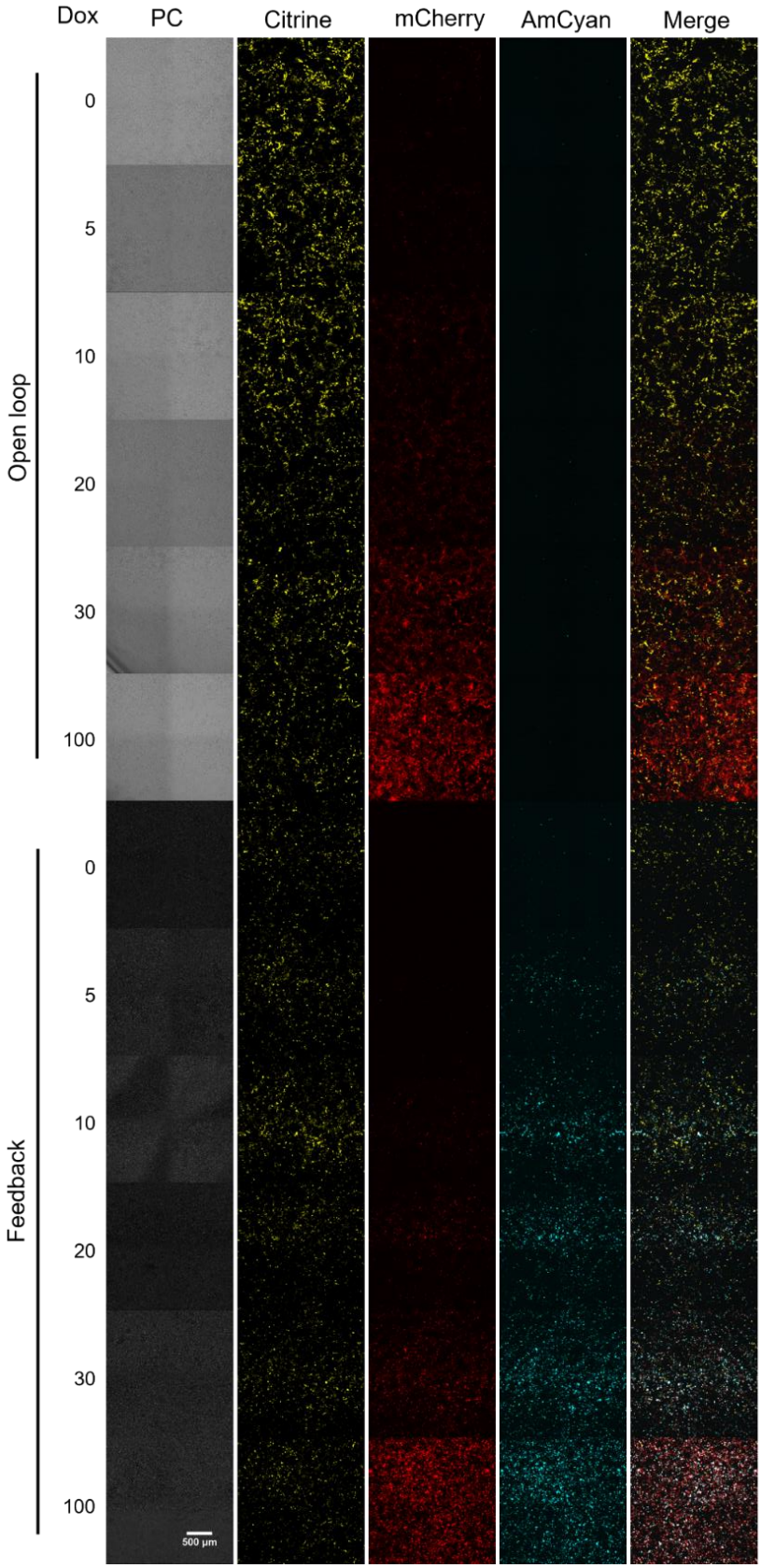

Figure 6: A montage of one replicates' microscopy images over all four channels as well as a merge of the three fluorescent channels over all doxycycline concentrations (given in ng/ml) for feedback- and open-loop. Exposure times of 300 ms was chosen for each of the fluorescent channels. Differences in brightfield (PC) images between open- and feedback-loop are due to the use of different microscope settings between plates.

Flow Cytometry Results

Flow cytometry recordings confirm what was seen in the microscopy images, as seen in figure 6. Both the open- and feedback-loop increase in mCherry-positive cells with higher doxycycline concentrations, which can be nicely see in the first column of the respective circuits in figure 6. Comparing the second column however, we see there is little to no increase in amCyan for the open-loop circuit, while there is a clear correlation for the feedback-loop. This is again demonstrated in the last column, with the open-loop values only increasing in the y-axis.

Looking at the integrated fluorescence data seen in figure 7, we again see the expected upwards trend for both circuits in mCherry and just the feedback-loop for the amCyan. However, we can also see a slight downward trend in the Citrine channel, especially for the feedback-loop. This could be due to the increase in metabolic burden at higher doxycycline concentrations, but this would require further testing to confirm. Either way, the downwards trend of the transfection control further accentuates the upwards trend in the other two channels.

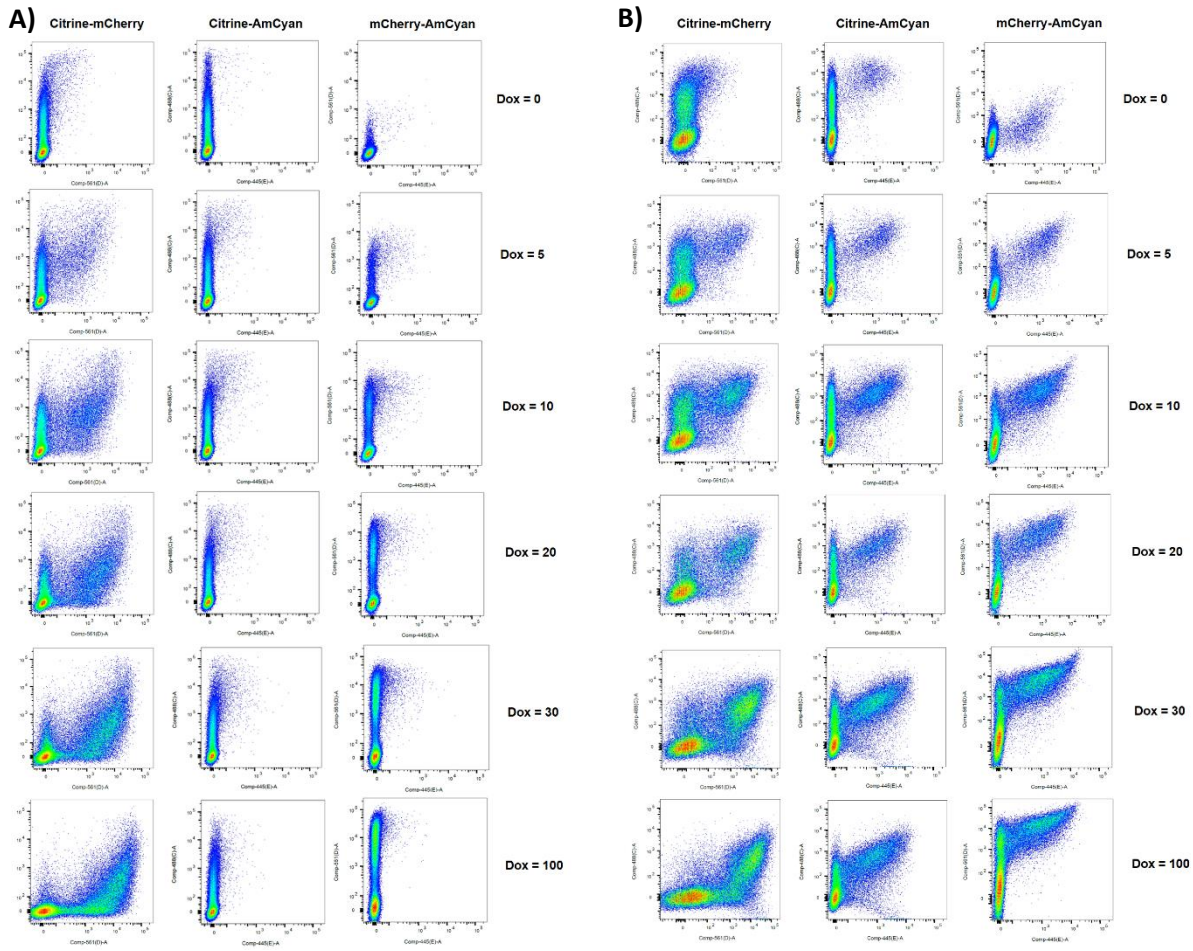

Figure 6: Representative fluorescence values from one replicate per doxycycline concentration of flow cytometry data. The fluorescence values plotted against each other are annotated above each column (y-axis – x-axis), and doxycycline concentrations are given in ng/ml. Plots are shown for both open- (A) and feedback-loop (B).

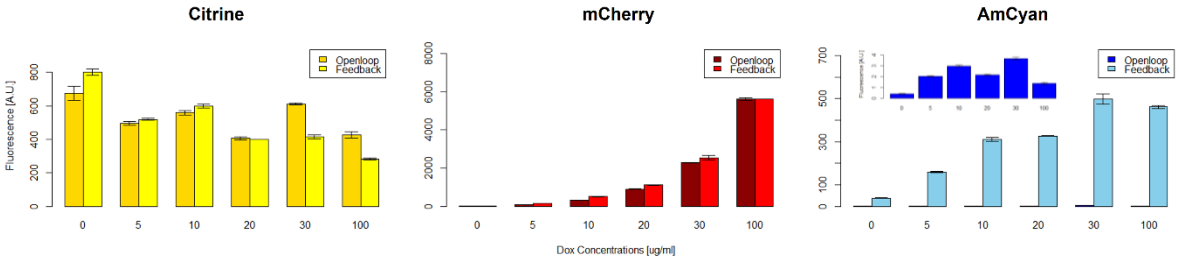

Figure 7: Integrated fluorescence values for each fluorescent protein over all dox concentrations (given in ng/ml), for both open- and feedback-loop. A close-up of open-loop amCyan values were added due to extremely low values compared to the feedback-loop.

Peak finding & simulation data

Looking at figure 8, the scatter plot of the bin 3 data follows the same trend as found in the FlowJo analysis in the previous chapter. The bimodality of this distribution is nicely demonstrated with the two peaks for each doxycycline concentration.

We can see a large jump in the upper peak for both circuits between 0 & 5 ng/ml doxycycline before evening out, with the open-loop even staying constant over higher dox concentrations. This is due to the fact that there is no activation at 0 doxycycline, leading us to expect single-peak distribution. The bimodal fit is therefore actually not ideal for this concentration. However, the lower peak still seems to be accurate (see figure 3), so we can ignore the upper peak for Dox=0. Other than this outlier, the peaks of the cell distributions are as expected.

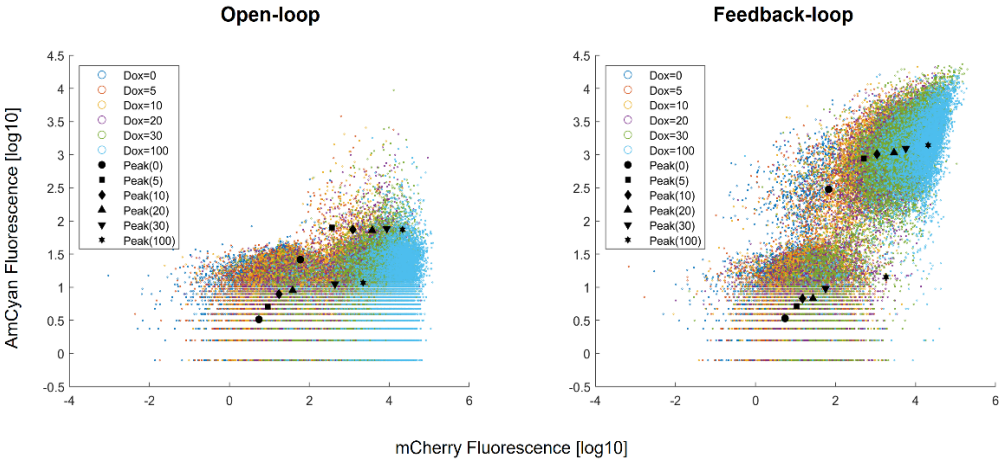

Figure 8: Single cell fluorescence data of bin 3 shown as a scatter plot on a log-scale. Peaks determined by the bimodal fit can also be seen as black points, two points of the same form always representing the high and the low peak of the fit.

To compare the experimental data to the model, deterministic simulations were run at different plasmid copy numbers and transcription rates of sensor plasmids with and without SOX10 and/or PIT2. The parameters for the simulation best fitting the experimental data, as seen in figure 9, was then chosen to conduct a stochastic and noisy simulation.

When comparing this simulated data, as seen in figure 10, to the experimental data in figure 8, we can see that the general form is similar, with some discrepancies. One big difference is the distribution of the Dox=0 samples. While the experimental shows strong overlap between this and the rest of the samples, the simulation shows a population almost entirely separated from the rest of the samples. One

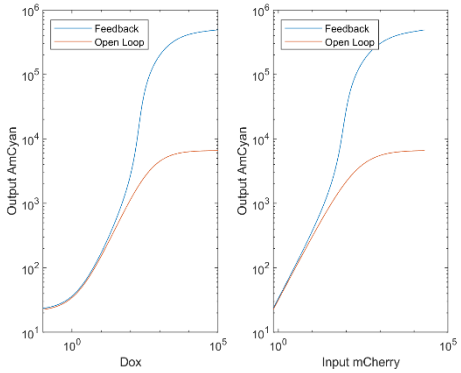

Figure 9: Deterministic simulations without noise of feedback- and open-loop.
Parameters: Plasmid copy numbers = 4, transcription rate of sensor i) with SOX10 or PIT2 = 0.0001 s^{-1}, ii) with SOX10 and PIT2 = 0.02

argument that could account for this observation is that we underestimate the leakiness values in the model, which was set at 1e-8 s^{-1}. This could lead to the strong 'shut-off' of sensor and output proteins which could be unrealistic in an experimental setting.
Looking at the simulated feedback-loop, we can see that the bimodality observed in the experimental data is reproducible in a simulation setting, thanks to a certain level of noise. It is however more strongly pronounced in the experimental data and can also be observed in the open-loop circuit (to a certain degree), which is not the case for the simulated open-loop data.

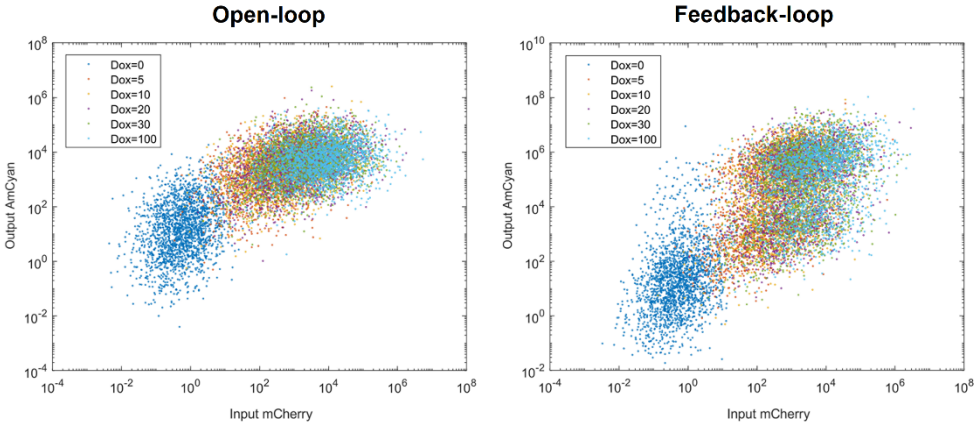

Figure 10: Stochastic simulation data shown as a scatter plot for both open- and feedback-loop.
Parameters: Noise = 0.6, simulation repeats = 2000

Conclusion & Discussion

In summary, we succeeded in reproducing the sensor module presented by Angelici et al. in 2016 [2], characterizing the input/output behaviour in HEK293 TetON cells. Several methods were used to introduce and characterize the corresponding circuits, including plasmid purification, lipofectamine transfection, automated microscopy & flow cytometry. The experimental data acquired was also compared to simulation data generated from the SimBiology model in Matlab.
For both the experimental and simulation data, a bimodal input/output response could be observed for the feedback-loop. There was however little to no increase of output for the experimental open-loop data, as well as not showing a bimodal response. To further characterize the open-loop circuit, higher levels of input/doxycycline could be used, until a noticeable increase in output would occur. This might however put a large metabolic strain on the cell containing the circuit.
These results nicely show the use of positive feedback loops in biology, elucidating a strong output response for only small amounts of input. Such characteristics can be used to create strong signal amplification and even toggle switches in the right situations.
In conclusion, we showed this sensor module, especially the feedback-loop circuit, to be a powerful tool to sense molecules such as transcription factors and encode and amplify this signal to be used further in downstream computations.

References

[1] Cameron, D., Bashor, C. & Collins, J. A brief history of synthetic biology. *Nat Rev Microbiol, 12*, 381–390 (2014). https://doi.org/10.1038/nrmicro3239

[2] Angelici, B., Mailand, E., Haefliger, B., & Benenson, Y. Synthetic Biology Platform for Sensing and Integrating Endogenous Transcriptional Inputs in Mammalian Cells. *Cell reports*, *16*(9), 2525–2537 (2016). https://doi.org/10.1016/j.celrep.2016.07.061